Journal of Polymers and the Environment
https://doi.org/10.1007/s10924-024-03306-5

ORIGINAL PAPER

Reprocessable Cross-Linked EVA/Silica Nanocomposites with Superior Mechanical Properties via One-Step and Scalable Reactive Blending

Haixin Nong[1] · Xiaopei Li[2] · Yongjie Zhang[1]

Accepted: 30 April 2024

Abstract

Organic/inorganic nanocomposites uniquely combine the dual advantages of inorganic nanomaterials and organic polymers. However, poor compatibility between inorganic nanoparticles and polymer matrices always arises as a huge obstacle to be addressed while designing and preparing high performance organic/inorganic nanocomposites. In situ surface grafting of ethylene–vinyl acetate copolymer (EVA) onto nanosilica and partial cross-linking of EVA via dynamic Si–O–C bonds with nanosilica as the core were simultaneously achieved via the transesterification reactions between the inherent Si–OH groups on the surface of nanosilica and the ester groups in EVA. The reactions were conducted thorough a one-step, simple and scalable reactive blending approach. The cross-linking reaction of EVA was evidenced by torque curves, FT-IR spectra and gel fraction testing. Uniform dispersion of silica particles in EVA matrix was observed for resulting EVA/silica nanocomposites due to surface modification of silica. Consequently, tremendous enhancement in mechanical properties of resultant EVA/silica nanocomposites were detected. Compared to the original EVA, the tensile strengths and tensile modulus of the EVA/silica nanocomposites increased by 72.5% and 37.8%, respectively, while the elongation at breaks of the EVA/silica nanocomposites remained as high as that of the original EVA. Additionally, the dynamic nature of Si–O–C cross-linkages enabled partially cross-linked EVA/silica nanocomposites to demonstrate exceptional reprocess ability and recyclability. This was evidenced by the sustained mechanical properties of the EVA/silica nanocomposites, which were still maintained even after undergoing three rounds of reprocessing.

Graphical Abstract

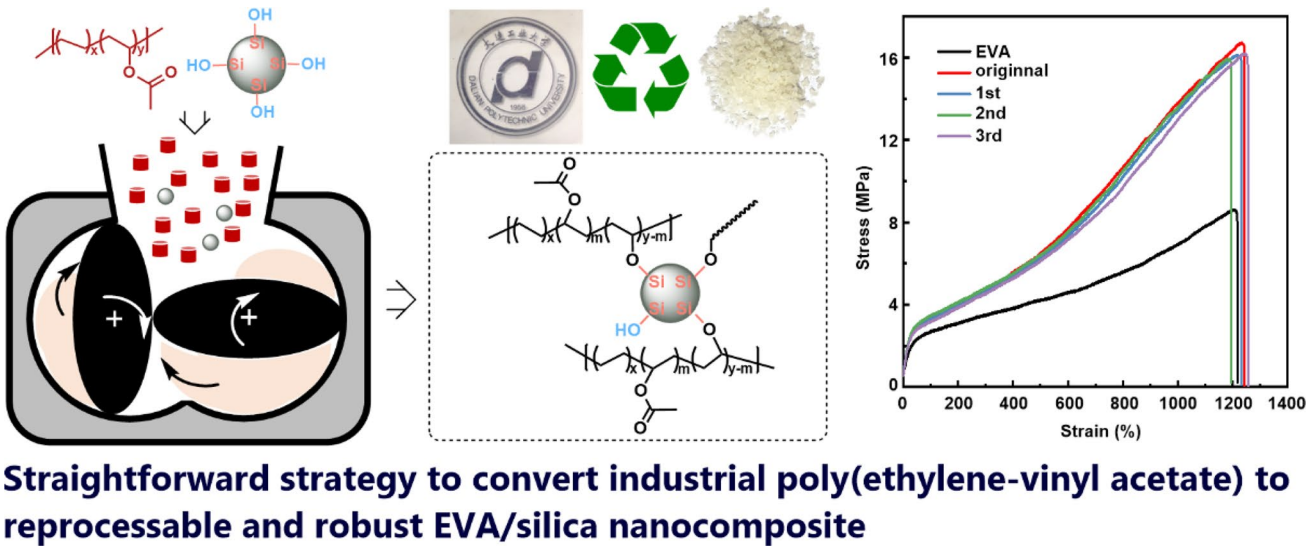

EVA/silica nanocomposites strengthened by dynamic cross-linking.

Extended author information available on the last page of the article

Published online: 01 June 2024

Keywords Polyolefins · Nanocomposites · Silicas · Recycling · Crosslinking

Introduction

Organic/inorganic nanocomposites are composed of organic polymer as the matrix and nanoscale inorganic particles dispersed in continuous polymer phase acting as the reinforcement [1–5]. Organic/inorganic nanocomposites can perfectly combine the thermostability, dimensional stability and mechanical strength of inorganic particles with the lightness, flexibility, processability and excellent dielectrical property of organic polymers to obtain superior properties over organic polymers, such as excellent mechanical, electrical, thermal, and optical properties [6, 7]. The dimensions, surface tension and distribution of nanoparticles are crucial for the improvement in the properties of nanocomposites. [8, 9] For polyolefin-based nanocomposites, the high surface energy of inorganic fillers and in-compatibilization between fillers and non-polar polyolefin commonly lead to poor dispersion of nanoparticles in polyolefin matrix. [10–12]. The aggregation of nanoparticles will result in significant reductions in the mechanical properties of resultant composites, failing to satisfy the requirements for specialty applications [13, 14]. Consequently, the establishment of a favorable interface between nanoparticles and the polyolefin matrix, along with achieving nanoscale dispersion of nanoparticles in the polyolefin matrix, are vital for preparing high-performance composites [15–18].

A plethora of methods has been developed to facilitate the effective dispersion of nanoparticles within polymer matrix, including in situ polymerization, in situ sol–gel generation of nanoparticles, surface modification of nanoparticles, utilization of compatibilizer and the use of polymer-coated nanoparticles [11]. Among many approaches, the surface modification of nanoparticles emerges as the appealing strategy to address the challenge of achieving homogeneous dispersion of nanoparticles within the polymer matrix while promoting good interfacial interactions. In particular, surface modification of nanoparticles via polymer grafting is an effective method to prepare polymer nanocomposites with excellent performance, which involves grafting polymer chains onto the surface of nanoparticles in the form of covalent bonds, and then further compositing them with polymer (or grafting reaction and composite process are carried out simultaneously) [19–23]. For semicrystalline polymers such as polyolefin, the grafted polyolefin chains on the nanoparticles can not only entangle but also co-crystallize with the polyolefin matrix, thus effectively preventing the agglomeration of nanoparticles. Yudhanto et al. reported on the feasibility and efficiency of preparing polyethylene grafted silica nanoparticles through surface-initiated polyhomologation, as well as their application in polyolefin nanocomposites [24]. Zhao et al. reported the preparation of polyethylene grafted α-zirconium phosphate which maintains the exfoliation of α-zirconium phosphate during subsequent blending with the polyethylene matrix and guarantees the preparation of high performance polyolefin nanocomposites [25]. Zhang et al. showed that short polyethylene chains grafted onto the surface of carbon nanotubes could promote the homogeneous dispersion of carbon nanotubes in polyethylene matrix [26]. Despite the favorable outcomes achieved with the aforementioned methods for nanoparticle modification, traditional approaches are frequently hindered by complex procedures, high expenses, and limited practicality.

Dynamic covalent bonds exhibit remarkable reversible cleavage and formation under specific conditions. Through the introduction of dynamic covalent bonds into the polymer networks, specific covalently cross-linked polymer materials unprecedentedly achieve reproducible processing properties, such as reprocessability, self-healing, and recyclability [27–29]. Among numerous dynamic covalent bonds that have been widely utilized to design vitrimers, self-healing materials and other functional soft materials, Si–O–C dynamic bond is of unique interests as it holds the potentials to directly link the organic polymers and inorganic nanoparticles such as silica and layered silicates, which usually possess sufficient reactive Si–OH groups on their surfaces. Two decades ago, Bounor-Legaré et al. reported that a special transesterification reaction occurs between the pendant aliphatic ester groups (–OC–O–C) in ethylene–vinyl acetate copolymer (EVA) and silyl ester (Si–O–C) groups in organosiloxane, which straightforwardly obtains cross-linked EVA with Si–O–C cross-linkages [30–32]. It has been recently found that Si–O–C bonds can undergo reversible cleavage and reconstruction, thus making the cross-linked polymers exhibit ductility and reprocess ability under suitable conditions [33, 34]. Recently, we found that, taking advantages of the transesterification between aliphatic ester and silyl ester groups, EVA-derived vitrimers could be facilely obtained via direct cross-linking of an industrial EVA with commercial organosiloxane through mild reactive blending [33]. Our results showed that EVA-derived vitrimers with dynamic and thermally stable Si–O–C cross-linkages exhibit significantly enhanced thermal and mechanical properties, as well as excellent reprocessability and recyclability (Scheme 1A). Inspired by the above results, we envision that abundant Si–OH groups inherently on the nanosilica surface may undergo transesterification reactions with ester group in EVA, generating EVA nanocomposites cross-linked

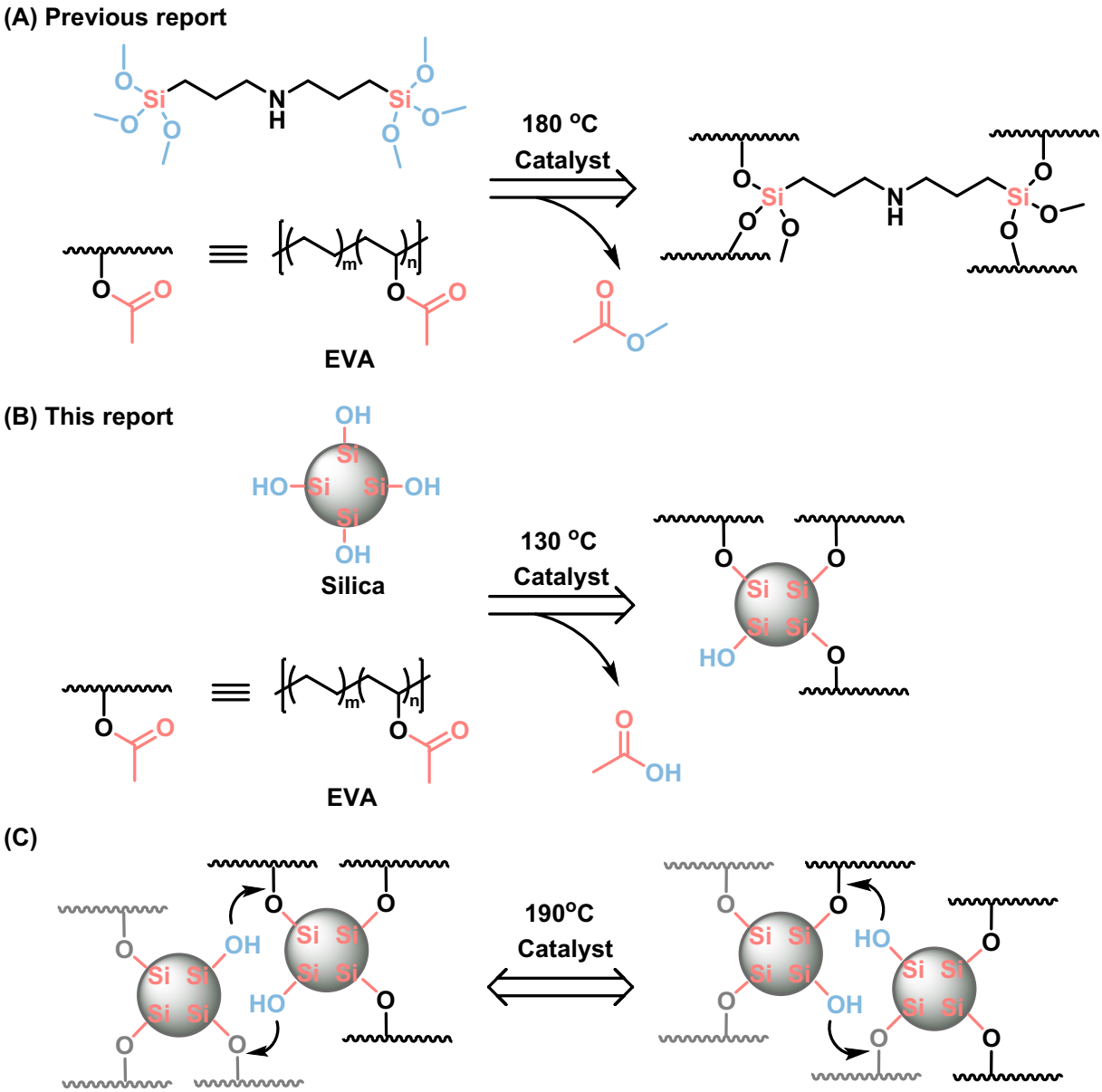

Scheme 1 One-step preparation procedure of EVA-derived vitrimer (**A**) and EVA/silica nanocomposite (**B**); **C** Proposed rearrangement process of network via dynamic Si–O–C bond exchange in EVA/silica nanocomposite

and enforced by nanosilica (Scheme 1B). Furthermore, thanks to the well-known dynamic feature of Si–O–C cross-linkages, the reprocessability and recyclability of resultant EVA/silica nanocomposites are anticipated.

Experimental Sections

Materials

Ethylene vinyl acetate copolymer (EVA; trade grade: UE 2825; vinyl acetate content: 28 wt%) kindly provided by Jiangsu Sierbang Petrochemical Co Ltd., tetrabutyl titanate (TT-01, 99%) from Innochem, antioxidant AO225 from Linyi Sanfeng Chemical, and silica nanoparticles (average diameter of 50 nm) from Shanghai Macklin Biochemical Co., Ltd. were used as received.

Preparation and Reprocessing of EVA/Silica Nanocomposites

In a typical procedure, 40 g EVA, 0.4 g antioxidant AO225, 2 g silica nanoparticle, and 0.6 mL tetrabutyl titanate (TT-01) were mixed up in a ZJL-200 torque rheometer to prepare

nanocomposites. EVA, silica, catalyst and antioxidant were first pre-mixed in a ziplock bag by hand with 5 mL dichloromethane and then dried before being added to the mixer for blending, which ensures that the silicas are uniformly dispersed in the pre-heated EVA particles. The reaction temperature and the torque speed were set to be 130 °C and 45 rpm, respectively. After reactive blending for 60 min, the obtained samples nanocomposites were subsequently molded into sheets with 1 mm depth for further testing using a QLB-50D/Q plate vulcanizing press machine under 5 MPa at 190 °C for 120 min.

For comparison, EVA/silica nanocomposites without catalyst were also prepared following the same procedure. The EVA/silica nanocomposites prepared with and without TT-01 were denoted as X–Y and X–Y w/o, respectively; where X was the phr of silica applied and Y was the reaction temperature.

To illustrated the reprocessability, smashed particles of EVA composites were remolded into 1 mm deep sheets in a QLB-50D/Q flat vulcanizer. The remolding process was conducted under 5 Mpa at 190 °C for 30 min.

Gel Fraction Testing

A weighed specimen of approximately 0.3 g was placed in a Soxhlet extractor by wrapping the specimen in filter paper and then extracted by boiling xylene for 12 h.

The extraction allowed uncross-linked polymer chains to dissolve into the hot solvent, while leaving the cross-linked polymers in the swollen state. The solvent in the swollen polymers was removed completely by heating the samples at 70 °C for 24 h in a vacuum chamber. The weight before and after testing was recorded to calculate the gel fraction as follows:

$$\text{Gel fraction} = \frac{\text{final weight}}{\text{initial weight}} \times 100\% - W_{\text{silica}}$$

where W_{silica} refers to the calculated mass ratio of silica in as-prepared nanocomposites.

Characterization

Torque Rheometer

The torque rheometer curves were collected directly during the blending process of all nanocomposites by a ZJL-200 torque rheometer.

FTIR

Attenuated total reflection Fourier transform infrared (ATR-FTIR) spectra of all samples were recorded by an iS50 infrared spectrometer (Thermo Fisher Scientific Inc., USA) using a resolution of 4 cm^{-1}. The testing wavenumber ranges from 4000 to 500 cm^{-1}.

SEM

The surface micromorphology of the samples was observed by field emission scanning electron microscopy (SEM) (JSM-7800F, JEOL, Japan). The EVA nanocomposites were fully freeze-hardened by immersing them in liquid nitrogen and then snapped off immediately.

Tensile Test

The aforementioned sample sheets were cut into dogbone shaped tensile specimens with dimensions approximately to be 2 mm × 1 mm × 20 mm. The tensile tests were performed on an AGX-X10 universal material testing machine (Shimadzu, Japan) at ambient temperature with a pull rate of 10 $mm \cdot min^{-1}$. Clean breaks were observed for all testing specimens. At least three specimens of each sample were tested and the average values of tensile properties were calculated to determine the tensile properties of each sample.

Melt Flow Rate

Melt flow rate (MFR) of EVA and composites were performed using a melt flow rate measurer (FBS-400BT) according the standard of GB/T 3682-2000. The test temperature and the load weight were 190 °C and 2.16 kg, respectively.

DSC

The crystallization and melting behaviors of all samples were determined using a a differential scanning calorimeter (DSC, Q200, TA Instruments, USA). The samples sealed by the aluminum pan were first heated from room temperature to 140 °C at 20 $°C \cdot min^{-1}$ to eliminate the thermal history. Subsequently, the samples were cooled to − 30 °C at 10 $°C \cdot min^{-1}$ to obtain the crystallization curves and kept at − 30 °C for 3 min. Then, the samples were reheated to 140 °C at 10 $°C \cdot min^{-1}$ to obtain the melting curves. The nitrogen flow rate was set to be 50 mL min^{-1}.

TGA

The thermal gravimetric analyses of all polymers were performed to determine the thermostability using a thermal gravimetric analyzer (SDTQ600, TA Instruments, USA). The tests were performed at a heating rate of 10 $°C \cdot min^{-1}$ from 50 °C to 650 °C in a N_2 atmosphere.

Results and discussion

Torque Rheometer Curves

According to our previous report [33], TT-01 can serve as an efficient catalyst to catalyze the transesterification reactions between ester groups in EVA and alkoxy groups. Inspired by this finding, TT-01 was chosen as the catalyst for the cross-linking reactions between ester groups in EVA and silanols on silica. The torque rheometer was employed to monitor the torque change during the cross-linking process of EVA in an internal mixer. The sample was coded by the phr of nanosilica and compounding temperatures (see Sect. "Preparation and Reprocessing of EVA/Silica Nanocomposites"). As depicted in Fig. 1, the torque of all samples quickly reached a peak point at the beginning and then diminished sharply in tens of seconds, which was recognized the melting process of EVA. The torque of sample 1–130 w/o went to a steady value around 5 N·m while the torque of its counterpart with catalyst TT-01 climbed up to nearly 30 N·m and then decreased slowly to about 15 N·m at 3000 s. Obviously, the introduction of TT-01 elicits a notable escalation in torque values, which can be ascribed to the cross-linking reaction between EVA and SiO_2. Samples with higher silica contents (i.e., 2–130 and 5–130) showed similar torque curves as 1–130, revealing the cross-linking reactions. The torque of 5–130 was generally lower than those of 1–130 and 2–130 at 500 ~ 2500 s, which may be attributed to the lubricating effect of silica on the EVA matrix [34].

FTIR Analysis

The FTIR spectra explicitly confirm the transesterification between ester groups in EVA and silanols on the surface of silica. As shown in Fig. 2, characteristic absorption peaks corresponding to bonds in backbone and side groups of EVA were clearly assigned (Table S1), such as the C–H stretching (2916, 2850 cm^{-1}) and C = O stretching (1738 cm^{-1}). Other peaks corresponding to C–O–C stretching (1250 cm^{-1}), C–H bending (1467 cm^{-1}, in methylene; 1371 cm^{-1}, in methyl), and C–C rocking (720 cm^{-1}). In the FTIR spectra of EVA/silica nanocomposites, the characteristic stretching absorption of Si–O-Si in SiO_2 appeared at 1107 cm^{-1}, while new peak emerged at approximately 1082 cm^{-1} was assigned to be the absorption peak associated with Si–O–C bonds. Therefore, the cross-linking reaction of EVA by SiO_2 was reconfirmed by FTIR analyses.

Gel Fraction Test

Cross-linked polymers possess three-dimensional network structures, resulting in good solvent resistance. Swelling tests were conducted to determine the solvent resistance and gel contents of EVA/silica nanocomposites. EVA, 1–130 w/o and 5–130 w/o were completely dissolved in hot xylene, while EVA/silica nanocomposites prepared with catalyst only swelled in hot xylene, proving that EVA/silica nanocomposites prepared with catalyst have excellent solvent resistance as they can maintain covalent cross-linking without dissociation in organic solvents (Table S2 and Figure S2). Initially, the reaction temperatures were set to be 170 ~ 190 °C, the common processing temperatures for EVA. The results revealed that the gel contents were relatively

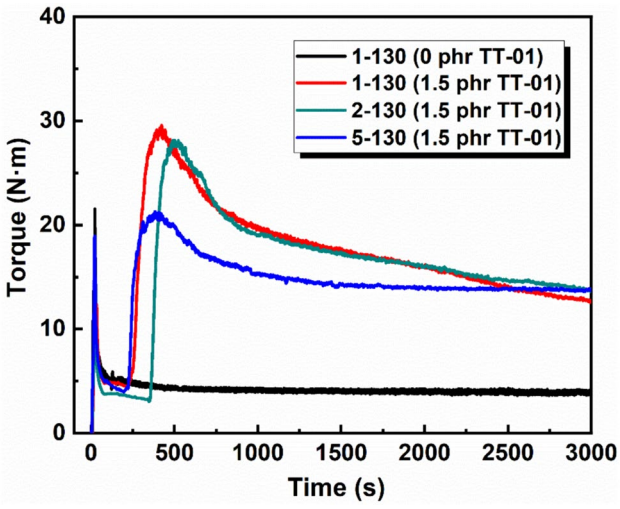

Fig. 1 Typical torque curves of EVA/silica nanocomposites with varying silica contents (reaction temperature: 130 °C; catalyst, TT-01)

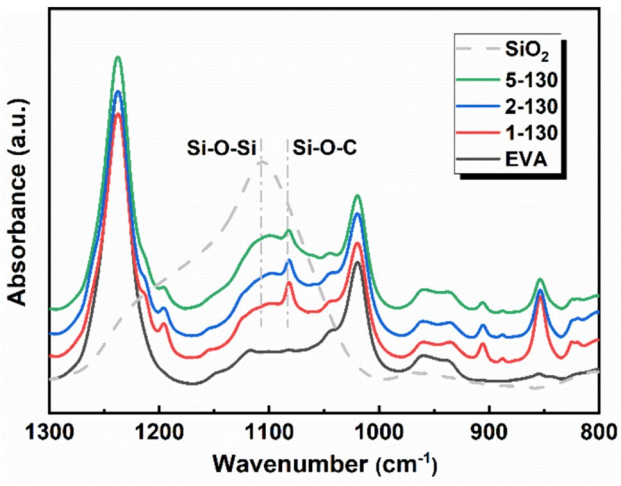

Fig. 2 Typical FTIR spectra of EVA resin, silica and EVA/silica nanocomposites generated in the presence of catalyst (Full scale spectra shown in Figure S1)

low (< 26 wt%) and decreased as the temperatures raised. Therefore, the cross-linking reactions were further explored at lower temperatures (110 ~ 160 °C). The gel fractions of 2–110 and 2–120 were lower than 8 wt%, suggesting that the cross-linking reactivity between silica and EVA was minimal at lower temperatures. When the reaction temperature increased to 130 °C, the gel fraction of 2–130 reached to a highest level, being 31.3 wt%. As the reaction temperature continued to increase, the gel fractions of the EVA/silica nanocomposites decreased, indicating that the degree of cross-linking of the EVA composites was highly dependent on the reaction temperature. The reasonable explanations could be that the silanols on silica surface may condense into siloxane groups at elevated temperatures, which consequently lowers the reaction rates between silanols on silica surface and ester in EVA [35, 36]. The gel fractions of 1–130 and 5–130 were 31.2 wt% and 32.3 wt%, respectively, indicating that the contents of silica exhibited minor influences on the gel fractions of EVA/silica nanocomposites.

Melt Flow Rate

To further validate the cross-linking reactions, MFR tests were performed for pristine EVA and nanocomposites (Fig. 3). The MFR of EVA reached to 23.73 g/10 min, while MFR of all EVA/silica nanocomposites prepared with TT-01 notably decreased. Meanwhile, all nanocomposites with varying SiO_2 contents showed a strong correlation between increasing reaction temperatures and declining flow ability. This trend can be attributed to a decrease in cross-linking degrees of nanocomposites as reaction temperatures rises. As indicated in gel fraction tests, nanocomposites prepared at lower reaction temperatures (e.g., 2–130) have higher cross-linking degrees, and thus, lower MFR values are expected. In fact, the MFR values of 1–130, 2–130 and 5–130 decreased to lower than 0.1 g·10 min^{-1}, clearly indicating a significant decrease in flow ability of EVA composites and implying the occurrence of dynamic cross-linking of EVA.

Morphology of EVA/Silica Nanocomposites

The morphologies of EVA/silica nanocomposites prepared with and without catalyst were examined by SEM analyses. The SEM micrographs of 5–130 w/o, which contains unmodified silica nanoparticles (Fig. 4A), demonstrated the agglomeration and heterogeneous distribution of silica nanoparticles in EVA matrix due to the high tendency to adhere to each other for silica nanoparticles. In contrast, only small particles were found in 5–130 and 1–130 that contain polymer surface-grafted silica nanoparticles (Fig. 4B, C), proving that the silica nanoparticles were uniformly dispersed in the EVA matrix. EDS analysis revealed that the dispersion of Si element in EVA/silica nanocomposite 5–130 was much more homogenous than that in 5–130 w/o (Figure S3), which further evidenced the uniform dispersion of silica in EVA/silica nanocomposite 5–130. The well dispersion of silica particles in EVA matrix demonstrates that good compatibility between inorganic and organic phases was achieved due to the grafting of EVA to silica through covalent bonds.

Mechanical Properties

Table S3 and Figure S4 compared the mechanical properties of EVA/silica nanocomposites samples with and without catalyst TT-01. The mechanical properties (tensile strength, e.g.) of 1–130 w/o and 5–130 w/o slightly increased compared to pristine EVA, yet still much lower than those of their counterparts 1–130 and 5–130. Therefore, the following discussion focuses on the nanocomposites prepared with catalyst. The stress–strain curves and the corresponding mechanical properties data of the EVA/silica nanocomposites samples prepared with catalyst are presented in Fig. 5 and Table 1, respectively.

The mechanical properties of EVA/silica nanocompoosites prepared at 110 °C and 120 °C showed minimal changes compared to linear EVA, suggesting that the reactivity between silica and EVA is low at lower temperatures. When the reaction temperature increased to 130 °C, the mechanical properties of nanocomposites significantly

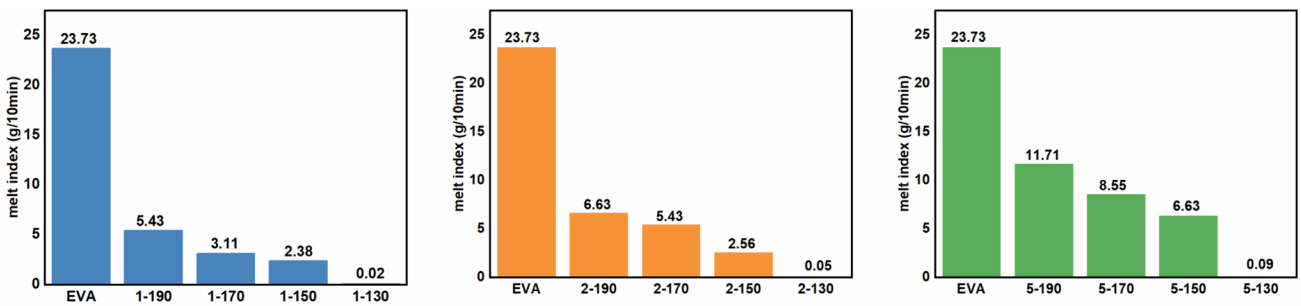

Fig. 3 Melt flow rate of EVA and EVA/silica nanocomposites

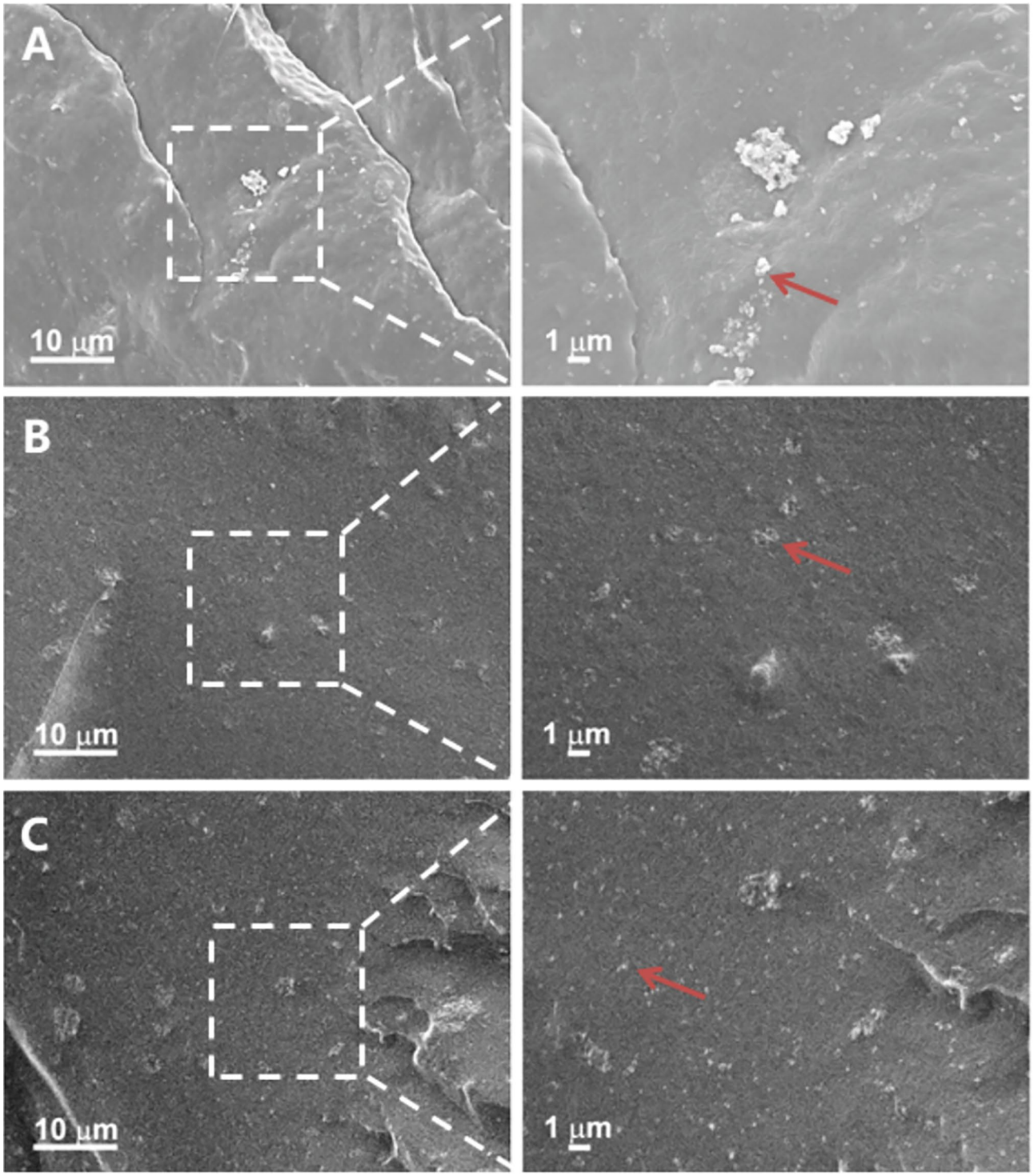

Fig. 4 SEM micrographs of fracture faces of **A** 5–130 w/o, **B** 5–130 and **C** 1–130

improved. For instance, sample 1–130 achieved a tensile strength of 16.78 MPa, a tensile modulus of 6.63 MPa, and an elongation at break of 1312%, which are clearly superior to pristine EVA. The increment in tensile strength, tensile modulus and elongation at break of 1–130 are 72.5%, 37.8% and 1.7% compared to those of EVA, respectively. Similar results were also observed for EVA/silica nanocomposites with higher silica contents (i.e., 2 phr and 5 phr). The enhancement in mechanical properties was partially attributed to the grafting of EVA onto silica surface, which

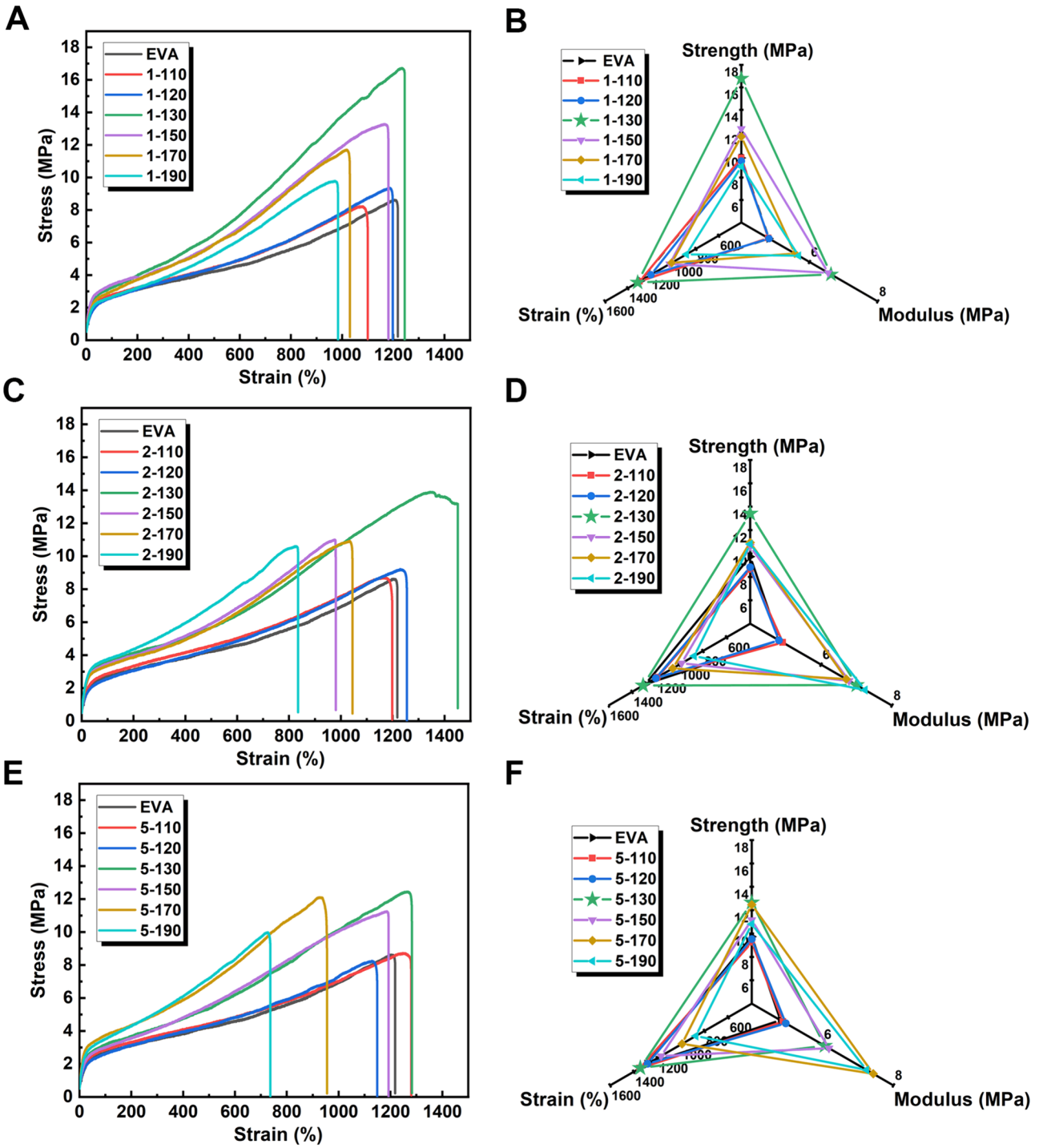

Fig. 5 Typical engineering stress–strain curves and radar charts of EVA and nanocomposites prepared under various conditions

promises the good compatibility between silica and EVA matrix and consequently promotes the uniform distribution of silica into the EVA matrix. Meanwhile, the cross-linking of EVA via Si–O–C linkages at the interface of EVA and silica may also considerably enhance the tensile strength and tensile modulus of EVA/silica nanocomposites.

When the reaction temperature continues to increase, both tensile strengthes and elongations at break of resultant nanocomposites generally exhibited a decreasing trend. For example, compared to 1–130, the elongation at break of sample 1–190 decreased from 1312 to 883% and the tensile strength decreased from 16.78 MPa to 8.97 MPa.

Table 1 Tensile properties of EVA and composites with different temperature and phr of SiO_2

Sample	SiO_2 (phr)	Temperature (°C)	Tensile strength (MPa)	Elastic modulus (MPa)	Elongation (mm/mm)
EVA		–	9.73 ± 0.63	4.81 ± 0.10	12.88 ± 1.10
1	1	110	9.73 ± 1.30	4.79 ± 0.12	12.95 ± 1.69
2		120	9.46 ± 0.81	4.81 ± 0.53	11.95 ± 1.01
3		130	16.78 ± 1.29	6.63 ± 0.75	13.12 ± 0.96
4		150	12.33 ± 1.05	6.55 ± 0.69	10.30 ± 1.30
5		170	11.63 ± 0.82	5.57 ± 0.26	10.13 ± 0.62
6		190	8.97 ± 0.88	5.68 ± 0.76	8.83 ± 1.04
7	2	110	8.63 ± 0.49	4.92 ± 0.28	11.87 ± 0.26
8		120	8.83 ± 1.27	4.81 ± 0.66	11.99 ± 1.99
9		130	13.41 ± 1.00	7.00 ± 1.64	13.06 ± 1.55
10		150	10.59 ± 1.35	6.79 ± 0.32	9.81 ± 1.20
11		170	10.94 ± 0.12	6.71 ± 0.24	10.55 ± 0.28
12		190	10.81 ± 1.07	7.24 ± 0.64	8.74 ± 0.85
13	5	110	9.24 ± 0.45	4.88 ± 0.05	13.48 ± 0.60
14		120	9.53 ± 1.04	4.96 ± 0.62	12.82 ± 1.17
15		130	12.66 ± 1.05	6.06 ± 0.54	13.44 ± 1.48
16		150	11.17 ± 0.20	6.18 ± 0.40	11.68 ± 0.28
17		170	12.47 ± 0.71	7.43 ± 0.83	9.90 ± 0.88
18		190	10.81 ± 1.07	7.24 ± 0.64	8.74 ± 0.85

Other identical conditions: 1. Reaction time, 1 h; 2. Molding time and temperature, 2 h and 190 °C; 3. The mass ratio of EVA/TT-01/AO225: 100/1.5/1.

This phenomenon can be attributed to the potential thermal aging of EVA at elevated temperatures, which can lead to EVA molecular chain breakage, oxidation, and other chemical reactions that degrade the mechanical properties of EVA nanocomposites. The content of SiO_2 will also affect the tensile strength and strain of the EVA composites. The correlation between silica contents and mechanical properties of nanocomposites were depicted in Figure S5 and Table S4. With the silica contents increased from 0.5 to 5 phr, the tensile strength and tensile modulus of EVA composites initially increased and then decreased. The increase in the dosages of silica would initially enhance the cross-linking degrees of EVA, thus in favor of enhancement in mechanical properties of nanocomposites. However, excessive silica may lead to a decrease in the homogeneity of the dispersion, resulting in declines in the mechanical properties of nanocomposites. The mechanical properties of EVA/silica nanocomposites and several EVA composites reported in literatures were compared in Figure S6, demonstrating the superiority of EVA/silica nanocomposites. Meanwhile, traditional approaches to EVA/silica composites often require labor- and time-consuming preparation steps, such as the dispersion of silica in polymer solutions and the surface modification of silica. By contrast, the proposed approach herein is featured by its simplicity, efficiency, scalability and low cost.

Reprocessability

The enhancement in mechanical properties of EVA/silica nanocomposites was greatly attributed to the partial cross-linking of EVA by silica. Meanwhile, the dynamic feature of Si–O–C cross-linkages promises the topological rearrangement of the cross-linked network and the reprocessability of EVA/silica nanocomposites at elevated temperatures. The reprocessability of EVA/silica nanocomposites with 1–130 as a representative sample was evaluated by testing the mechanical properties of reprocessed nanocomposites. The reprocessing involves crushing the sample into small fragments and then molding them at 190 °C and 5 Mpa for 30 min. As shown in Table 2 and Fig. 6A, the Young's modulus, tensile strengths, and elongations at break for samples recycled for 1, 2, and 3 times were found to be nearly identical, indicating that 1–130 exhibited excellent reprocessability and recyclability and that EVA/silica nanocomposites can be recycled and reprocessed effectively without obvious losses in their mechanical properties. Figure 6B revealed that the reprocessed 1 mm deep EVA/silica nanocomposites specimen showed good transparencies. Dynamic Si–O–C cross-linkages can undergo reversible exchange reactions that facilitate the transformation and reorganization of cross-linking structure in the EVA/silica nanocomposites (Scheme 1C), which thus enables the reprocessability of

Table 2 Tensile properties of composite after multiple reprocessing cycles

Sample	Tensile Strength (MPa)	Elastic modulus (MPa)	Elongation (mm/mm)
1–130-original	16.78 ± 1.29	6.63 ± 0.75	13.12 ± 0.96
1–130-1st	16.13 ± 0.49	6.37 ± 0.14	12.44 ± 0.89
1–130-2nd	16.04 ± 0.27	6.74 ± 0.04	11.83 ± 0.26
1–130-3rd	16.27 ± 0.69	6.65 ± 0.41	12.13 ± 0.59

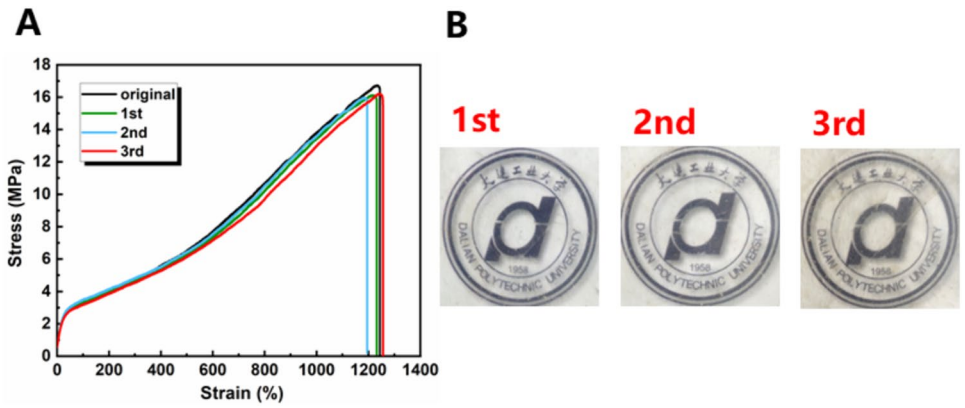

Fig. 6 **A** Strain–stress curves for original 1–130 and the reprocessed 1–130 samples × 1, × 2, and × 3; **B** Digital pictures of 1–130 samples after being mashed and reprocessed for three times

cross-linked EVA/silica nanocomposites and makes the mechanical integrity of EVA/silica nanocomposites well maintained after repeating the processing cycles. Sample 1–130 with the second highest gel fraction (31.2 wt%) was found to possess good reprocessability and optimal mechanical properties. Other EVA/silica composites with lower gel fractions may also have good reprocessability. However, their mechanical properties are inferior to 1–130. Therefore, the reaction conditions for 1–130 are considered to be the optimal processing conditions for achieving the desired balance between mechanical performance and reprocessability.

Thermal Properties of EVA Composites

The crystalline behaviors of EVA and nanocomposites were analyzed by DSC. Figure S7 revealed that the EVA composites exhibited melting processes that closely resembled those of EVA. As shown in Table S5, the T_m and ΔH_m of nanocomposites were slightly lower than those of EVA (74.12 °C, 24.21 J/g), especially for samples 2–130 and 5–130. Cross-linking of EVA may restrict the mobility of the chains, making it difficult for the chains to rearrange and crystallize, and thus resulting in lower T_m and ΔH_m. The DSC results are consistent with the gel fraction and MFR results. Compared to its counterparts prepared at higher temperatures, samples 2–130 and 5–130 with higher gel fractions, and thus higher cross-linking degrees, exhibited lower MFR and lower T_m and ΔH_m.

TGA technique was employed for the thermal stability assessments of EVA and representative nanocomposites. The TGA curves and data collected are shown in Figure S8 and Table S6, respectively. The decomposition temperatures at 5% weight loss ($T_{5\%}$) for pristine EVA, 1–130, 2–130, and 5–130 samples were determined to be 335.77 °C, 339.65 °C, 336.17 °C and 331.87 °C, respectively. The TGA data demonstrated that the observed $T_{5\%}$ of nanocomposites initially increased compared to that of EVA, and decreased monotonously as the silica contents increased. The decrement in $T_{5\%}$ of nanocomposites may be partially attributed to the weight loss of silica due to dehydration.

Conclusion

In conclusion, we reported a novel strategy for preparing robust and reprocessable EVA/silica nanocomposites through the transesterification reaction between Si–OH groups inherent on the surface of silica and the ester groups in EVA. Through a one-step and industrially adaptable reactive blending process, simultaneous surface modification of nanosilica and partial cross-linking of EVA via dynamic cross-linkages were successfully achieved, which resulted in homogenous dispersion of nanosilica in EVA matrix and considerable enhancement in mechanical properties of EVA/silica nanocomposites. Last yet not least, the mechanical properties of EVA/silica nanocomposites were well maintained after repeated reprocessing, indicating that EVA/silica nanocomposites partially cross-linked via dynamic Si–O–C exhibited excellent reprocessability. The superior properties of EVA/silica nanocomposites, as well as their straightforward, scalable and low-cost preparation procedure, give us the confidence in the industrial application of this technique

in the near future. Further research is on-going in our lab to realize the vision.

Supplementary Information The online version contains supplementary material available at https://doi.org/10.1007/s10924-024-03306-5.

Author Contributions Y. Zhang and X. Li conceived the study and designed the experiments. H. Nong performed most of the experiments. Y. Zhang and H. Nong wrote the manuscript. X. Li helped in discussing the results and polishing the language. All authors reviewed the manuscript.

Funding The work was supported by a grant from the Department of Education of Liaoning (General Program, Grant No. LJKMZ20220902).

Data Availability The authors declare that the data supporting the findings of this study are available within the paper and its Supplementary Information files. Should any raw data files be needed in another format they are available from the corresponding author upon reasonable request.

Declarations

Competing Interests The authors declare no competing interests.

References

1. Meer S, Kausar A, Iqbal TJP-PT (2016) Engineering, attributes of polymer and silica nanoparticle composites: a review. Polym Plast Technol Eng 55:826–861
2. Paszkiewicz S, Pypeć K, Irska I, Piesowicz E (2020) Functional polymer hybrid nanocomposites based on polyolefins: a review. Processes 8:1475
3. Rahman A, Al-Zahrani S, Ali I, Eliethy R (2011) A review of the applications of nanocarbon polymer composites. NANO 6:185–203
4. Baig N, Kammakakam I, Falath W (2021) Nanomaterials: a review of synthesis methods, properties, recent progress, and challenges. Mater Adv 2(6):1821–1871
5. Harito C, Bavykin DV, Yuliarto B, Dipojono HK, Walsh FC (2019) Polymer nanocomposites having a high filler content: synthesis, structures, properties, and applications. Nanoscale 11(11):4653–4682
6. Mallakpour S, Naghdi M (2018) Polymer/SiO_2 nanocomposites: production and applications. Prog Mater Sci 97:409–447
7. Sharma AK, Bhandari R, Aherwar A, Rimašauskienė R (2020) Matrix materials used in composites: a comprehensive study. Mater Today: Proc 21:1559–1562
8. Alonso YN, Grafia AL, Castillo LA, Barbosa SE (2021) Active packaging films based on polyolefins modified by organic and inorganic nanoparticles. React Funct Polym Vol Three Adv Mater. https://doi.org/10.1007/978-3-030-50457-1_26
9. Dang ZM, Yuan JK, Yao SH, Liao RJ (2013) Flexible nanodielectric materials with high permittivity for power energy storage. Adv Mater 25(44):6334–6365
10. Peng Z, Li Q, Li H, Hu Y (2017) Polyethylene-modified nano silica and its fine dispersion in polyethylene. Ind Eng Chem Res 56(20):5892–5898
11. Zou H, Wu S, Shen J (2008) Polymer/silica nanocomposites: preparation, characterization, properties, and applications. Chem Rev 108(9):3893–3957
12. Kroll S (2023) Surface modification of ceramic materials. Surface-functionalized ceramics. Wiley, Hoboken, pp 85–118
13. Muthuraj R, Mekonnen T (2018) Carbon dioxide–derived poly (propylene carbonate) as a matrix for composites and nanocomposites: performances and applications. Macromol Mater Eng 303(11):1800366
14. Peng S, Yu Y, Wu S, Wang C–H (2021) Conductive polymer nanocomposites for stretchable electronics: material selection, design, and applications. ACS Appl Mater Interfaces 13(37):43831–43854
15. Baniasadi H, Seppälä J (2021) Novel long-chain aliphatic polyamide/surface-modified silicon dioxide nanocomposites: in-situ polymerization and properties. Mater Today Chem 20:100450
16. Kango S, Kalia S, Celli A, Njuguna J, Habibi Y, Kumar R (2013) Surface modification of inorganic nanoparticles for development of organic–inorganic nanocomposites—a review. Prog Polym Sci 38(8):1232–1261
17. Guan S, Li H, Zhao S, Guo L (2018) Novel three-component nanocomposites with high dielectric permittivity and low dielectric loss co-filled by carboxyl-functionalized multi-walled nanotube and $BaTiO_3$. Compos Sci Technol 158:79–85
18. Min C, Yu D, Cao J, Wang G, Feng L (2013) A graphite nanoplatelet/epoxy composite with high dielectric constant and high thermal conductivity. Carbon 55:116–125
19. Bounor-Legaré V, Cassagnau P (2014) In situ synthesis of organic–inorganic hybrids or nanocomposites from sol–gel chemistry in molten polymers. Prog Polym Sci 39(8):1473–1497
20. Zhang Y, Li Q, Wang W, Guo A, Li J, Li H (2017) Efficient and Robust reactions for polyethylene covalently grafted carbon nanotubes. Macromol Chem Phys 218(4):1600449
21. Huang Y, Zheng Y, Sarkar A, Xu Y, Stefik M, Benicewicz BC (2017) Matrix-free polymer nanocomposite thermoplastic elastomers. Macromolecules 50(12):4742–4753
22. Liu C-X, Choi J-W (2012) Improved dispersion of carbon nanotubes in polymers at high concentrations. Nanomaterials 2(4):329–347
23. Zhao N, Yan L, Zhao X, Chen X, Li A, Zheng D, Zhou X, Dai X, Xu F-J (2019) Versatile types of organic/inorganic nanohybrids: from strategic design to biomedical applications. Chem Rev 119(3):1666–1762
24. Alghamdi RD, Yudhanto A, Lubineau G, Abou-Hamad E, Hadjichristidis N (2022) Polyethylene grafted silica nanoparticles via surface-initiated polyhomologation: a novel filler for polyolefin nanocomposite. Polymer 254:125029
25. Zhao M, Wu H-M, Zhu Z, Wu J-L, Kang W-H, Sue H-J (2022) Preparation of polyethylene nanocomposites based on polyethylene grafted exfoliated α-zirconium phosphate. Macromolecules 55(8):3039–3050
26. Zhang Y, Li Q, Wang W, Guo A, Li J, Li H (2016) Efficient and Robust reactions for polyethylene covalently grafted carbon nanotubes. Macromol Chem Phys 218:1600449
27. Guerre M, Taplan C, Winne JM, Du Prez FE (2020) Vitrimers: directing chemical reactivity to control material properties. Chem Sci 11(19):4855–4870
28. Van Zee NJ, Nicolaÿ R (2020) Vitrimers: permanently crosslinked polymers with dynamic network topology. Prog Polym Sci 104:101233
29. Zheng J, Png ZM, Ng SH, Tham GX, Ye E, Goh SS, Loh XJ, Li Z (2021) Vitrimers: current research trends and their emerging applications. Mater Today 51:586–625
30. Bounor-Legaré V, Angelloz C, Blanc P, Cassagnau P, Michel A (2004) A new route for organic–inorganic hybrid material synthesis through reactive processing without solvent. Polymer 45(5):1485–1493
31. Bounor-Legaré V, Ferreira I, Verbois A, Cassagnau P, Michel A (2002) New transesterification between ester and alkoxysilane

groups: application to ethylene-co-vinyl acetate copolymer crosslinking. Polymer 43(23):6085–6092
32. Bounor-Legaré V, Monnet C, Llauro M-F, Michel A (2004) Ethylene-co-vinyl acetate copolymer crosslinking through ester–alkoxysilane exchange reaction catalyzed by dibutyltin oxide: mechanistic aspects investigated through model compounds by multinuclear NMR spectroscopy. Polym Int 53(5):484–494
33. Zhang J, Li X, Zhang S, Zhu W, Li S, Zhang Y, Hu Y, Zhou G (2023) Facile approach for the preparation of robust and thermally stable silyl ether cross-linked poly(ethylene-vinyl acetate) vitrimers. ACS Appl Polym Mater 5(10):8379–8386
34. Zhao Y, Qi X, Dong Y, Ma J, Zhang Q, Song L, Yang Y, Yang Q (2016) Mechanical, thermal and tribological properties of polyimide/nano-SiO_2 composites synthesized using an in-situ polymerization. Tribol Int 103:599–608
35. Pavan C, Santalucia R, Leinardi R, Fabbiani M, Yakoub Y, Uwambayinema F, Ugliengo P, Tomatis M, Martra G, Turci F, Lison D, Fubini B (2020) Nearly free surface silanols are the critical molecular moieties that initiate the toxicity of silica particles. Proc Natl Acad Sci 117(45):27836–27846
36. Mohanan S, Guan X, Liang M, Karakoti A, Vinu A (2023) Stimuli-responsive silica silanol conjugates: strategic nanoarchitectonics in targeted drug delivery. Small. https://doi.org/10.1002/smll.202301113

Authors and Affiliations

Haixin Nong[1] · Xiaopei Li[2] · Yongjie Zhang[1]

✉ Xiaopei Li
li_xp@dlpu.edu.cn

✉ Yongjie Zhang
yjzhang@dlpu.edu.cn

[1] School of Textile and Material Engineering, Dalian Polytechnic University, Dalian 116034, China

[2] Instrumental Analysis Centre, Dalian Polytechnic University, Dalian 116034, China